 doi:10.20944/preprints202109.0340.v1

Article

Long-term transplant effects of iPSC-RPE monolayer in immunodeficient RCS rats

Deepthi S. Rajendran Nair[1], Danhong Zhu[2], Ruchi Sharma,[3] Juan Carlos Martinez Camarillo[1, 4], Kapil Bharti[3], David R. Hinton[2], Mark S. Humayun[1,4], Biju B. Thomas[1, 4,*]

1. Department of Ophthalmology, Roski Eye Institute, Keck School of Medicine, University of Southern California, Los Angeles, CA 90033, USA.

2. Department of Pathology and Ophthalmology, USC Roski Eye Institute, Keck School of Medicine, University of Southern California, Los Angeles, CA, USA

3. Unit on Ocular and Stem Cell Translational Research, National Eye Institute, NIH, Bethesda, MD 20892, USA.

4. USC Ginsburg Institute for Biomedical Therapeutics, University of Southern California, Los Angeles, CA 90033, USA.

*Correspondence: biju.thomas@med.usc.edu, Tel: 323-442-5593

Abstract: Abstract: Retinal pigment epithelium (RPE) replacement therapy is evolving as a feasible approach to treat age-related macular degeneration (AMD). In many preclinical studies, RPE cells are transplanted as cell suspension into immunosuppressed animal eyes and transplant effects were monitored only short-term. We investigated the long-term effects of human iPSC derived RPE transplants in immunodeficient Royal College of Surgeons (RCS) rat model, in which RPE dysfunction lead to photoreceptor degeneration. iPSC-RPE cultured as polarized monolayer on nanoengineered ultrathin parylene C scaffold was transplanted into the subretinal space of 28-day old immunodeficient RCS rat pups and evaluated after 1, 4 and 11 months. Assessment at early time points showed good iPSC-RPE survival. The transplants remained as a monolayer, expressed RPE specific markers, performed phagocytic function and contributed to vision preservation. At 11-month post-implantation, RPE survival was observed only in 50% of the eyes that were concomitant with vision preservation. Loss of RPE monolayer characteristics at the 11-month time point was associated with peri-membrane fibrosis, immune reaction through activation of macrophages (CD 68 expression) and transition of cell fate (expression of mesenchymal markers). The overall study outcome supports the therapeutic potential of RPE grafts despite the loss of some transplant benefits during long-term observations.

Keywords: iPSC-RPE; retinal pigment epithelium; immunodeficient RCS rat; ultrathin parylene; retinal degeneration; retinal transplantation

 doi:10.20944/preprints202109.0340.v1

1. Introduction

Age-related macular degeneration (AMD), one of the most common causes of blindness in the developed world, is a degenerative disease of the retina often leading to progressive vision loss. Geographic atrophy, the advanced form of AMD, is characterized by dysfunction of retinal pigmented epithelium cells (RPEs) followed by degeneration of overlying photoreceptors leading to loss of central vision. At present no proven clinical treatments exist for the preservation or replacement of vulnerable RPE cells; however, RPE cell transplantation is perhaps the most obvious therapeutic option which has gained significant interest. In the early stages of AMD, although the RPE cells are dysfunctional, surviving photoreceptors and the inner retina that transmit visual signals to the brain remain functional, rendering a realistic possibility that replacing the degenerating RPE with functional young RPE will restore vision.

Potential sources of healthy RPEs are pluripotent cells derived from embryonic [1–4], or adult cell sources [5–9], which are differentiated into RPE cells by employing spontaneous or directed differentiation methods. Early-phase clinical trials by various research groups used embryonic stem cell derived RPE (ESC-RPE) for cell replacement that have already shown early signals of safety and potential efficacy [10–14]. Our team has demonstrated that human embryonic stem cell derived RPE (hESC-RPE) grown as a polarized monolayer on ultrathin parylene substrates can remain functional after transplantation in athymic nude rats[15] and in Royal College of Surgeons (RCS) rats[16,17], a model for RPE dysfunction. The product, termed California Project to Cure Blindness-RPE (CPCB-RPE1), is being assessed in an FDA–approved phase1/2a clinical trial (NCT 02590692) for advanced dry AMD and exhibits promising outcomes by improving visual activity [18].

The autologous induced pluripotent stem cell derived RPE (iPSC-RPE) transplantation is considered more advantageous as the chance of graft rejection issues can be minimized. Recent research focuses on generation of iPSC lines from adult cell sources, such as skin fibroblasts or peripheral blood mononuclear cells [5–9]. The four-year report of iPSC-RPE sheet transplant surgery for CNV (choroidal neovascularization- wet form of AMD) in one patient has been published recently [19]. Another major step forward is allogeneic transplantation of off-the-shelf available iPSC-RPE. Due to concerns regarding possible oncogenic mutations in the cell preparation, now the attention is focused towards personalised screening for mutations and development of autologous iPSC-RPE therapies including HLA matching [20,21]. A study by Sugita et al [22] aimed at examining the safety of six-loci HLA-matched allogeneic cell transplantation under local steroids. RPE cells grafted as a suspension into the patients subretinal space, survived in all five cases for more than two years [22]. These observations suggest that it is possible to manage the survival of iPSC-RPE, under immunosuppression. However, regenerative medicine is still in its infancy and the cells may behave differently in each individual. In the first iPSC-RPE transplantation clinical study [23,24], three aberrations in deoxyribonucleic acid (DNA) copy number (deletions) were observed in the cell preparation of the second patient that caused the study to end due to possible adverse effects.

Existing evidence indicate that delivery of cells as suspension may not consistently develop into a monolayer of RPE and that their survival rate will be low in long-term compared to RPE cells transplanted as a monolayer [15]. In many preclinical studies for geographic atrophy, the iPSC-RPEs were delivered into the subretinal space as bolus injection [26–29] and the animals were monitored for survival under immunosuppression only for a short period. Other studies in which iPSC-RPEs, transplanted as monolayer and maintained under immunosuppression regimes, were followed up for up to 5 months [25,19]. Published data suggests that a confluent polarized monolayer of iPSC-RPEs transplanted as a patch rather than as cell suspension can perform several basic functions of RPEs including phagocytosis of photoreceptor outer segments, renewal of visual pigment, and transport of metabolites [23,25]

Although transplantation of iPSC-RPE cells to replace the diseased RPE has been tested by several groups through preclinical studies and there are preliminary reports of ongoing preclinical studies, however, no major attempt has been made to perform an in depth analysis of the long-term viability and fate of the transplanted RPE. Based on previous reports from our group [17], progressive

deterioration of visual function after transplantation of ESC- RPE was evident during long-term observations. Monitoring cell survival and assessing long-term functional benefits of transplants are significant since the transplanted cells are exposed to a progressively degenerating environment and there may be immunological factors that can cause adverse effects.

In preclinical studies of RPE transplantation, one of the major factors that influence the long-term benefits is immune reaction and associated xenograft rejection. Sharma et al. [37] showed a 70% survival of subretinally transplanted human iPSC-RPE (hiPSC-RPE) cells up to 2.5 months post-implantation in immunosuppressed rodents. In the above study, systemic and resident innate immune responses in animal models were suppressed by using prednisone, doxycycline, and minocycline whereas the adaptive immune responses were suppressed using tacrolimus and sirolimus [25]. Del Priore et al, in 2003[39] demonstrated 'triple systemic' therapy with anti-inflammatory antibiotics to increase the survival of grafted RPE at four weeks post-implantation. But based on a previous report, immunosuppressants can alter visual function in RCS rats with depressed scores on behavioural and electrophysiological testing [38]. Hence, to minimize the complications associated with immunosuppressants, we used a newly developed immunodeficient RCS rat model characterised by an absence of T cells and lack of natural cell-mediated cytotoxicity [40]. The iPSC-RPE cells grown as a polarized monolayer on ultrathin perylene substrates were transplanted into the subretinal space of immunodeficient RCS rats. The transplant effects were assessed at various post-implantation time points (1 to 11 months after transplantation).

2. Materials and Methods

2.1. Human pluripotent stem cells generated from iPSCs

iPSC-RPE (frozen, passage 2 cells) generated from iPSCs, reprogrammed from healthy adult fibroblasts were obtained from Dr. Kapil Bharti, NIH, USA [30]. Briefly, hiPSC were seeded at 20,000 cells per cm^2 on Matrigel and grown in mTeSR1 in a 10% CO_2/5% O_2 incubator for 5 days. Afterward, they were transferred to a 5% CO_2/20% O_2 incubator and cultured for 5 additional days. At this point, the culture medium was switched to differentiation medium (DM) [30]. After day 10–15, cells were maintained in DM for 3 more weeks and then switched to RPE maintenance medium (RPEM) [30]. Differentiated cells were dissociated in Accumax (Sigma), plated at 250–300,000 cells per cm^2 and grown in RPEM. The passage 3 cells were used for transplantation experiments.

2.2. Preparation of polarized hESC-RPE implant on parylene membranes

Ultrathin parylene membranes (0.3-μm thickness supported on a 6.0-μm-thick mesh frame) made from parylene C were specially designed for implantation on rat retina (1.0 × 0.4 mm) [15,17] and used successfully for culturing iPSC-RPEs. These ultrathin membranes were coated with Matrigel (AMS Biotechnology, Frankfurt, Germany) and seeded with iPSC-RPE based on our previously established protocol [17]. The cells were grown to confluence for approximately 4 weeks before implantation. The final density of each implant was kept as approximately 2700 cells/ membrane [15].

2.3. Immunostaining of iPSC- RPE on parylene membrane

iPSC-RPE cells grown on Matrigel coated parylene were stained for RPE specific markers zonula occludens protein 1 (ZO-1), and RPE65, based on established protocols (17). Stained cells were mounted with anti-fading mounting medium (Invitrogen) and images were captured by confocal microscopy (FV1000 Confocal Microscope, Olympus, Centre Valley, PA, USA).

2.5. Animals

The Royal College of Surgeons (RCS) rat is an established model of retinal degeneration which has been mainly used for studying photoreceptor rescue with treatment at the age of 3-4 weeks. These rats develop a fully functional visual system which degenerates secondarily due to their dysfunctional RPE (MertK mutation), resulting in the loss of most photoreceptors at the age of 3 months. Immunodeficient RCS rats were produced from a cross between female homozygous RCS (RCS-p+/RCS-p+) and male athymic nude rats (Hsd: RH-Foxn1mu, mutation in the foxn1 gene; no T cells) as described previously [31]. All rats were maintained in an aseptic and temperature-controlled environment. All animals were included in accordance with the Association for Research in Vision

and Ophthalmology (ARVO) statement for the use of animals in research, and the Institutional Animal Care and Use Committee (IACUC) of USC.

2.6. Surgical procedure

Animals underwent surgery at postnatal day (P) 28. Anaesthesia was induced by intraperitoneal injection of ketamine (37.5 mg/kg) and xylazine (5 mg/kg). Only the left eyes were used for transplantation surgeries. Topical anaesthesia was administered with 0.5% proparacaine hydrochloride ophthalmic solution (Akorn, Inc., Lake Forest, IL). Pupils were dilated using ophthalmic solutions of 2.5% phenylephrine hydrochloride and 0.5% tropicamide (Akorn, Inc.). Once the conjunctiva is removed, a scleral incision was performed in the temporal superior quadrant followed by an anterior chamber paracentesis to reduce intraocular pressure. A 32-gauge needle was then inserted into the subretinal space through the scleral incision, and 5µl balanced salt solution (Alcon Laboratories, Inc., Fort Worth, TX) was injected to create a local retinal detachment. The implant held by forceps was introduced through the sub scleral space into the subretinal bleb. Clinical assessment as well as retinal imaging by optical coherence tomography (OCT) using Spectralis HRA+OCT device (Heidelberg Engineering, Heildeberg, Germany) were performed to confirm placement of the implant. The rats were then allowed to recover from anaesthesia in a thermal care incubator. Based on OCT images, 15 animals were selected for short-term experiments (1month and 4-month study group) and 15 animals were selected for 11-month study group.

2.8. Histopathology

Cohorts of rats were euthanized by intracardiac injection of euthasol (Virbac AH, Inc., Fort Worth, TX) at 1, 4- and 11-months post-surgery and eyes were processed for histology. Contralateral eyes were considered as controls. Whole eyes were fixed in Davidson's solution overnight, the cornea and lens were removed. Finally, the eye cups were embedded in paraffin and processed for sectioning (5-µm sections). Groups of consecutive slides were stained with haematoxylin and eosin (HE) for light microscopy. The HE stained slides were scanned and photographed using an Aperio Scanscope CS (Aperio Technologies, INL., Vista, CA, USA) microscope. Histological sections of cell-seeded membranes were evaluated to assess iPSC-RPE survival. The surgical placement was considered acceptable if more than 70% of the implant was located inside the subretinal area. Transplant survival was confirmed only if iPSC-RPE were observed in at least three consecutive sections based on light microscopy and immunostaining evaluations. Cell migration or dead cell aggregation was considered when pigmented cells or cell clumps were seen adjacent to the substrate and confirmed by immunohistochemistry. If no human/ RPE marker was found, the specimen was considered as non-surviving RPE clumps. The outer nuclear layer (ONL) integrity was evaluated for photoreceptor preservation in the transplanted area. Cellular reaction around the implants, observed by light microscopy, was assessed for the presence of macrophages or expression of glial cells. Adjacent sections of the implanted eye were processed for immunohistochemical analysis using the following antibodies as needed: human-specific cell surface marker (anti-TRA-1-85), a marker of differentiated RPE cells (anti-RPE65, a macrophage marker (anti-CD68), an astrocyte/Müller cell marker (anti-GFAP), mesenchymal markers (α Smooth muscle actin and Vimentin), photoreceptor phagocytosis marker (Rhodopsin), RPE binding protein (RBP1).

Details of the antibodies used are included in Table 1. For immunostaining, all slides were deparaffinized, rehydrated, and antigen retrieved (sodium citrate, pH 6.0). After staining, the slides were mounted with fluorescent-enhanced mounting medium with 4',6-diamidino-2-phenylindole (DAPI) (Vector Laboratory, Burlingame, CA, USA). Images were taken using the Ultra viewer ERS dual-spinning disk confocal microscope (PerkinElmer, Waltham MA, USA) equipped with a C-Apochromat (Carl Zeiss, Thornwood, NY, USA) ×10 high dry lens, a C-Apochromat ×40 water immersion lens NA 1.2, an electron multiplier charge-coupled device cooled digital camera (Hamamatsu Orce_ERCC [12 bit camera]; PerkinElmer, Waltham, MA, USA) or by using Keyence BZX-800 microscope. Images were captured and processed using PerkinElmer Velocity imaging software.

Antibodies	Purpose	Manufacturer	Catalog No	Dilution
TRA-1-85	Human marker	R&D Systems, Minneapolis, MN, USA	MAB3195	1:100
RPE65	RPE marker	Abcam	Ab231782	1:200
Rhodopsin	Rods	Abcam	Ab3267	1:100
CD68	Microglia	Abcam	ab201340	1:300
Vimentin	Mesenchymal marker	Abcam	ab137321	1:300
GFAP	Reactive glial cells	Invitrogen	MA5-12023	1:500
α Smooth muscle actin	Mesenchymal marker	Abcam	ab5694	1:250
Goat anti-mouse IgG conjugated with Rhodamine	Secondary antibody	Jackson Immuno Research, West Grove, PA, USA	115-025-146	1:500
Goat anti-rabbit IgG conjugated with FITC	Secondary antibody	Abcam	Ab150081	1:500
Ki67	Proliferation marker	Abcam	Ab16667	1:500
Donkey Anti-Mouse lgG H&L	Secondary Antibody	Abcam	Ab7003	1:500
Donkey Anti-Rabbit lgG H&L	Secondary Antibody	Abcam	Ab150063	1:500

Table 1. List of antibodies used for immunostaining

2.9. Superior colliculus electrophysiology

Electrophysiological mapping of the superior colliculus (SC) was performed at approximately 11-month post-surgery based on an established protocol followed in our laboratory [7, 39, 40]. Based on OCT screening, 8 rats (8/15) were selected for SC experiments. Rats dark-adapted overnight were anesthetized by intraperitoneal injection of xylazine/ketamine. The gas inhalant anaesthetic (1–2.0% isoflurane) was administered via an anaesthetic mask (Stoelting Company, Wood Dale, IL, USA). Rats were mounted in a stereotactic apparatus; a craniotomy was performed, and the SC was exposed. Multi-unit visual responses were recorded extracellularly from the superficial laminae of the SC using custom-made tungsten microelectrodes. For SC mapping, the responses were recorded from approximately 30 different SC locations. At each recording location, approximately 10 presentations of a full-field strobe flash (1300 cd m22, Grass model PS 33 Photic stimulator, W. Warwick, RI, USA), positioned 30 cm in front of the rat's eye, were delivered to the contralateral eye. An interstimulus interval of 5 seconds was used. The neural activities were recorded using a digital data acquisition system (Power lab; ADI Instruments, Mountain View, CA, USA) 100 milli seconds before and 500 milli seconds after the onset of the stimulus. All responses at each site were averaged. Blank trials, in which the illumination of the eye was blocked with an opaque filter, also were recorded at each site.

 doi:10.20944/preprints202109.0340.v1

2.10. Optokinetic testing

Optokinetic (OKN) testing was performed at 4 months and 11-month post transplantation using a previously described protocol [17]. To record OKN responses, two tablet screens were used to display the OKN stimuli consisting of high contrast black and white stripes generated using 'OKN Stripes Visualization Web Application', a freely available software (http://mdds.nyc/okn-stripes-visualization). A clear plexiglass holder was used to restrain the rat and keep its head continuously exposed to the tablet screen. A micro camera attached to the top of the rat holder recorded the head-tracking responses during clockwise (1 minute) and anticlockwise (1 minute) stripe rotations. Visual acuity was tested by changing the stripe width at 0.5 decrements. Video recordings were evaluated to compute the head-tracking scores by two separate investigators who were both masked to the experimental condition. The OKN responses at various spatial frequencies were assessed based on presence or absence of a clear head-tracking and or based on the duration of head-tracking.

2.11. Statistical Analysis

Statistical comparisons were made using GraphPad Prism software (GraphPad Software Inc., La Jolla, CA). The Paired *t* test was used for analysing the OKN data. The remaining data was analysed using Student *t* test or by Analysis of Variance (ANOVA) followed by appropriate post hoc test. For all comparisons, the significance level was determined at $p < 0.05$.

3. Results

3.1. Human iPSC-RPE cells can grow as a polarized monolayer over ultrathin parylene membrane and demonstrate high-purity and RPE marker expression

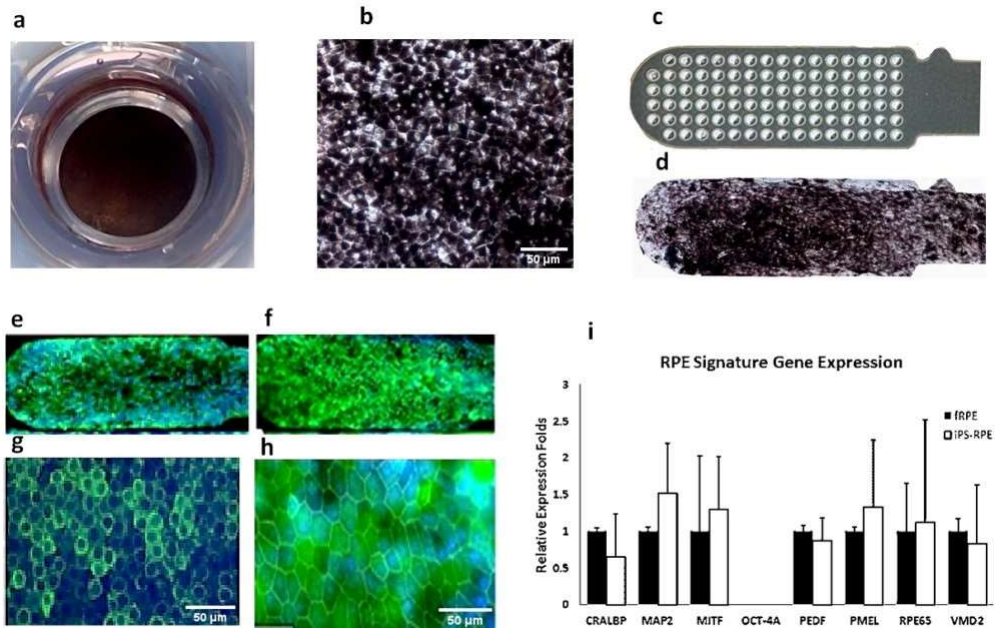

Figure 1. iPSC-RPE grown as polarized monolayer over parylene substrate. (a) iPSC-RPE polarized monolayer cultured on 24 well transwell insert, (b) enlarged view of iPSC-RPE monolayer, (c) ultrathin parylene membrane without cells, (d) iPSC-RPE grown as polarized monolayer on parylene membrane, (e) low magnification (10X) image stained for RPE 65 showing the whole implant, (f) ZO-1 expression, enlarged view of expression of RPE 65 (e), and ZO1 (f), (i) Quantitative measurement of RPE signature gene expression in iPSC-RPE on parylene membrane. iPSC-RPE cells expressed RPE signature genes similar to levels of expression in fetal RPE (fRPE). OCT-4, an undifferentiated embryonic stem cell marker, was not detectable in both fetal fRPE and iPSC-RPE.

 doi:10.20944/preprints202109.0340.v1

iPSC-RPE cells (Fig1.a,b) cultured on Matrigel coated ultrathin parylene substrate were expanded as a polarized confluent monolayer (Fig. 1,d) and expressed RPE 65 and ZO-1 as evidenced by immunocytochemistry (Fig.1.e,f,g,h). Quantitative PCR of iPSC-RPE monolayer grown on parylene have shown that the cells expressed similar levels of RPE signature genes as that of fetal RPE (fRPE). OCT-4, an undifferentiated embryonic stem cell marker, was not detectable in both fRPE and iPSC-RPE (Fig.1.i). This study demonstrated that iPSC-RPE can be grown as a polarized monolayer on ultrathin parylene similar to our previous hESC-RPE implants [17].

3.2. iPSC-RPE implant survival and functionality assessed by short-term in vivo experiments in immunodeficient RCS rats (1- and 4-month study)

After the transplantation surgery, OCT imaging was performed to screen the animals for proper implant placement (Fig 2.a.b.c). Animals with the implant placed as a flat sheet adjacent to the Bruch's membrane were selected for further analysis. Histological analysis at 1-month post-implantation showed presence of well pigmented, intact iPSC-RPE cell layer attached to the parylene substrate in all transplanted eyes. No major signs of

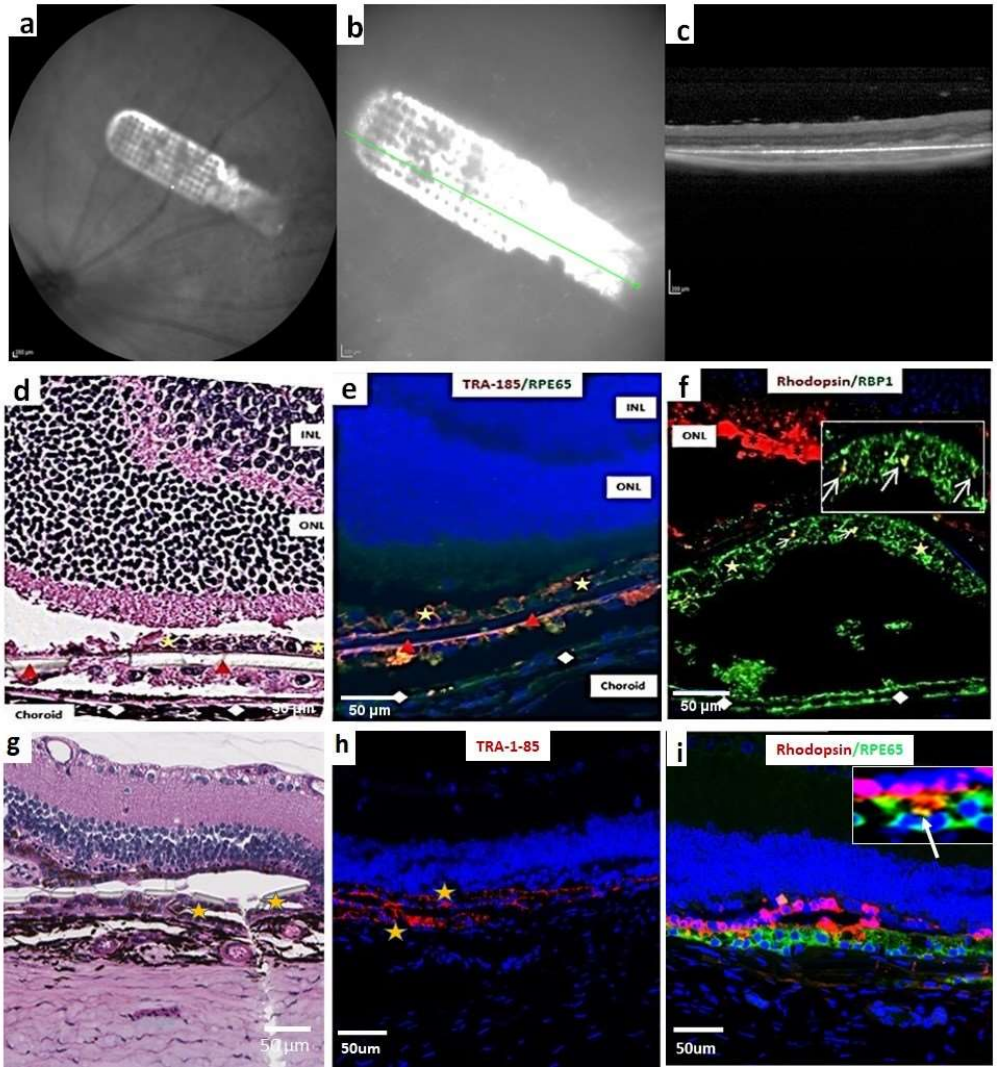

Figure 2. Short-term assessment of iPSC-RPE implant survival and functionality, in immunodeficient RCS rats. (a) iPSC-RPE implants observed during fundus examination of immunodeficient RCS rats at 1-month post-implantation (b) enlarged view, (c) vertical OCT b-scan image through the

 doi:10.20944/preprints202109.0340.v1

transplant area, (d) HE image showing subretinal implant placement. The choroidal layer that appears to be separated from the remaining retina is considered as a histologic artifact. Yellow asterisk-iPSC-RPE cells, (e) transplant is identified by TRA-1-85 (human specific marker, red) and RPE65 (green) expression, (f) Rhodopsin (red) and retinol-binding protein (RBP1, green) staining to demonstrate that implanted iPSC-RPE can phagocytose photoreceptor outer segments (white arrows). Inset is a higher magnification of the above area. Red arrowhead- parylene substrate; white rhombus- endogenous rat RPE, (g) HE image showing subretinal implant 4 months after transplantation, (h) transplant at 4 months is identified by TRA-1-85 (human specific marker, red). (i) rhodopsin (red) and RPE 65 (green) staining was used to show that implanted iPSC-RPE can phagocytose photoreceptor outer segments (yellow rhombus) at 4 months after transplantation. Inset is a higher magnification of the transplant area indicating phagocytosis (white arrow).

inflammation was observed in any of the implanted animals. A majority of the retinas (92.0%) maintained basic retinal architecture without noticeable structural changes. Histological analysis revealed that transplanted cells survived very well evidenced by TRA -1- 85 (human specific marker) expression and retinol-binding protein expression (Fig 2.e, f). Transplants in which iPSC-RPEs were present on the lower surface of the parylene membrane also showed good survival (Fig. 2e). At 1-month time point, the expression of CD68 (macrophage marker) and GFAP (retinal glial marker) were not observed in the transplant area (supplementary fig.1) or in the area outside the transplant (data not shown). The cells retained RPE 65 expression and human marker expression (Tra-1-85) without any evidence of mesenchymal marker expression (vimentin and α-smooth muscle actin, see supplementary Fig.2). Good survival of iPSC-RPE implants were also observed at 4-months post-implantation (Fig 2.g-i). Based on rhodopsin staining, the survived cells performed phagocytic function (Fig 2.i). The absence of immunological markers comparable to the control group point to the absence of detectable chronic inflammation induced by xenografts.

3.3. In vivo assessment of long-term transplant effects in immunodeficient RCS rats (11month study)

Evaluation of histology images from serial sections at 11-month post-implantation showed the presence of transplanted RPE in seven eyes (7/15). Out of these seven eyes, four eyes retained well-intact RPE monolayer structure. Immunostaining showed rhodopsin containing phagosomes in the transplanted RPE. This was more prominent in those eyes in which better preservation of iPSC-RPE monolayer structure was observed (Fig.3c). In the remaining three eyes, the cells appeared as clumps (Fig.3 e, f) out of which only 2 eyes retained RPE65 expression. There was no Ki 67 expression in the implanted areas suggesting absence of proliferative cells. Photoreceptor outer nuclear layer (ONL) preservation was evident in almost all the eyes in which strong RPE65 expression was noticed (Fig.3 c, f). Complete loss of transplanted cells was noticed in 8 (8/15) eyes.

 doi:10.20944/preprints202109.0340.v1

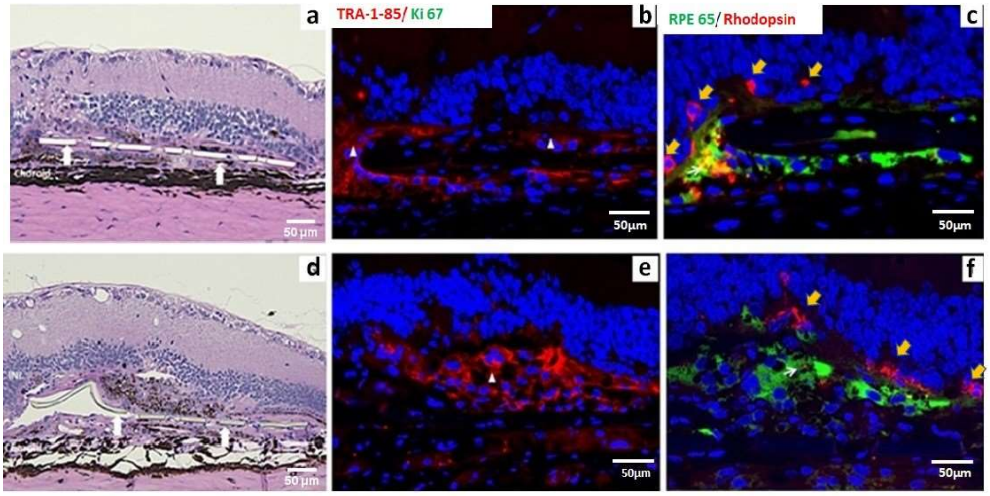

Figure 3. Representative HE and immunostaining images of immunodeficient RCS rats implanted with iPSC-RPE monolayer assessed at 11-month post implantation. Large white arrows (a, d) point to the parylene membrane. (a-c) retina containing iPSC-RPE monolayer, (d-f) retina with iPSC-RPE appeared as multiple cell layers or cell clumps. TRA-1-85 (white triangle in b, e) and RPE65 expression were used for identifying iPSC-RPE. Absence of Ki67 expression indicates absence of proliferative cells (b, e). Rhodopsin immunostaining is used to identify photoreceptor survival (yellow arrows in figure c, f). Rhodopsin containing phagosomes are found in the transplanted iPSC-RPE denoted by white arrows (c, f). Phagocytic activities were prominent in those eyes in which monolayer structure was better preserved (c).

ONL preservation was not observed in these eyes in which iPSC-RPE survival was absent. Presence of fibrosis was noticed in the majority of the above eyes (Fig.4 a, b). A summary of the histological result of 11-month post-implantation study is given in Table 2.

iPSC-RPE implant status			RPE65			Phagocytosis			Fibrosis/inflammation		
No cells or cells died	Presence of intact monolayer	Cells developed into clumps, no intact monolayer	++	+	-	++	+	_	++	+	-
8	4	3	4	2	9	0	4	11	2	4	9

Table 2. Summary of the histological result for iPSC-RPE implantation in immunodeficient RCS rats (11-month post implantation)

Expression of CD68 and GFAP were used to analyse inflammatory and glial reactions to donor tissues. GFAP was strongly expressed in the ganglion cell layer, inner nuclear layer and the choroid area but this was absent in the transplant area (Fig.4.c). CD68 positivity observed in some of the

 doi:10.20944/preprints202109.0340.v1

implanted eyes suggests inflammatory reactions associated to transplantation (Fig 4.d). To validate cell loss associated to the loss of tight junctions and consequent loss of cell-cell contact and cell-matrix contact, the tissue was tested for classic EMT markers- α smooth muscle actin (α SMA) and vimentin. Interestingly, in those implants in which RPE expression was absent or feeble, there was a strong expression of α smooth muscle actin (Fig 4.e) and vimentin (Fig 4.f) was noticed.

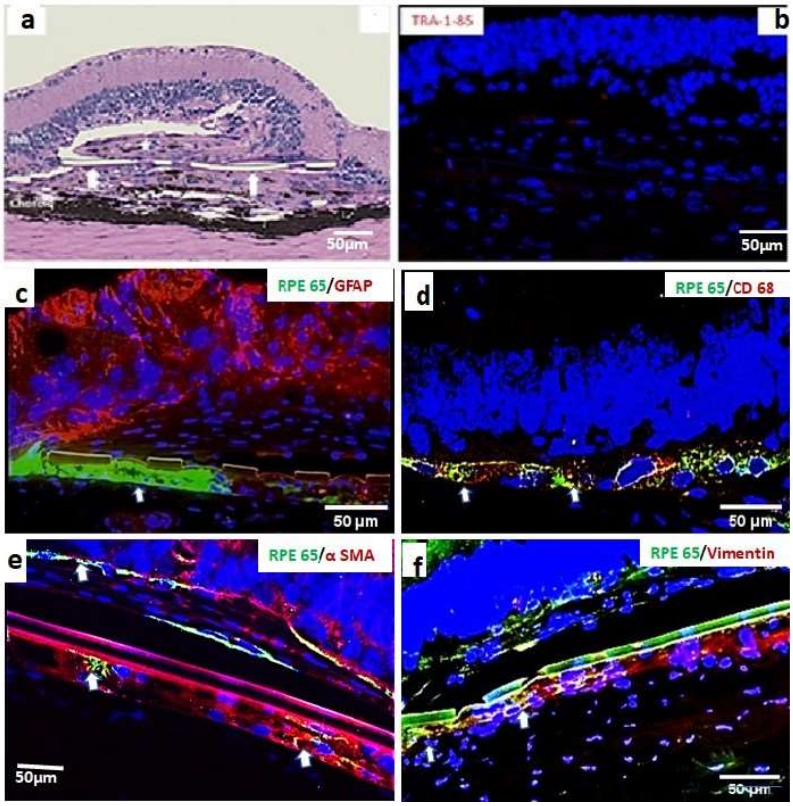

Figure 4. Representative HE and immunostaining images of immunodeficient RCS rat retinas implanted with iPSC-RPE monolayer assessed at 11 months post-implantation. Presence of fibrosis, immunoreactivity, and epithelial-mesenchymal transition (EMT) were assessed. (a) retina with no survived iPSC-RPE showing signs of inflammation and peri-membrane fibrosis indicated by white asterisk. (b) absence of TRA-I-85 staining. (c) retinas showing RPE65 expressing iPSC-RPE cells (white arrows) labelled for GFAP (glial cells), (d) CD68 (macrophages/microglia), (e) expression of classical mesenchymal markers α smooth muscle actin α SMA and vimentin (f). Images in which iPSC-RPE monolayer appears to be present below the parylene membrane is either due to orientation difference in the implant placement or due to the survival of the RPE on the lower side of the parylene membrane.

3.4. Preservation of low light level visual responses in the superior colliculus (SC) of iPSC-RPE implanted rats at 11-month post-implantation

iPSC-RPE implanted immunodeficient RCS rats were subjected to SC luminance threshold mapping (Fig 5). Electrophysiological mapping of the SC allowed for correlation of the response area in the SC with the location of the implant placement in the eye based on established retinocollicular map properties (41). Age-matched normal Long Evans (LE) rats showed visual activity from all over the SC (Fig 5 a). Among transplanted rats, visual preservation was observed only in 5 rats (5/8).

 doi:10.20944/preprints202109.0340.v1

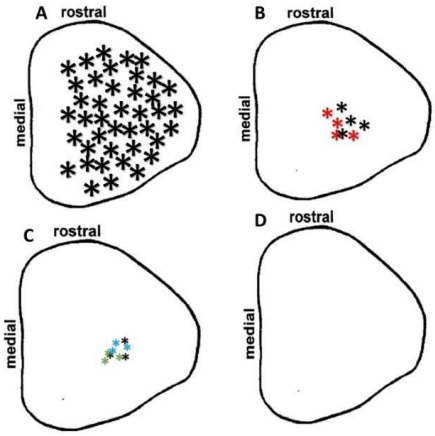

Figure 5. Visual activities recorded from the SC of 11-month-old immunodeficient RCS rats. *Map properties of SC-evoked responses from individual rats are represented by colored asterisks. Larger asterisks show higher light sensitivity in the SC. (A) Age-matched normal rat (B) *Rat # 6005 and *Rat # 6012 (C) *Rat # 6001, *Rat # 6006 and *Rat # 6011. Based on morphological examination, all these rats showed surviving iPSC-RPE in the retina (see Table 3). (D) No light evoked visual activity was observed in the remaining transplanted rats and age-matched control RD rats.*

Visually evoked activities in these rats was observed only in a small SC area corresponding to the implant placement in the eye. Visual activities were robust (higher light sensitivity) in two of the above rats (Fig 5b) whereas only weak visual activity (lower light sensitivity) was recorded in the remaining 3 rats (Fig 5c). No light-evoked visual activity was observed in the SC of age-matched non-transplanted rats (Fig 5 d). All the 5 rats that showed SC visual activity showed presence of transplanted RPE in their eyes (Table 2). No correlation was observed between the light sensitivity threshold and the degree of transplant survival.

3.5. Optokinetic (OKN) responses in iPSC-RPE implanted rats

Based on OKN data, visual improvement in the iPSC-RPE implanted eyes were observed at 4 months post-transplantation (Fig 6). However, when tested at 11-month time point, no measurable OKN responses were observed in any of the iPSC-RPE implanted rats (data not shown).

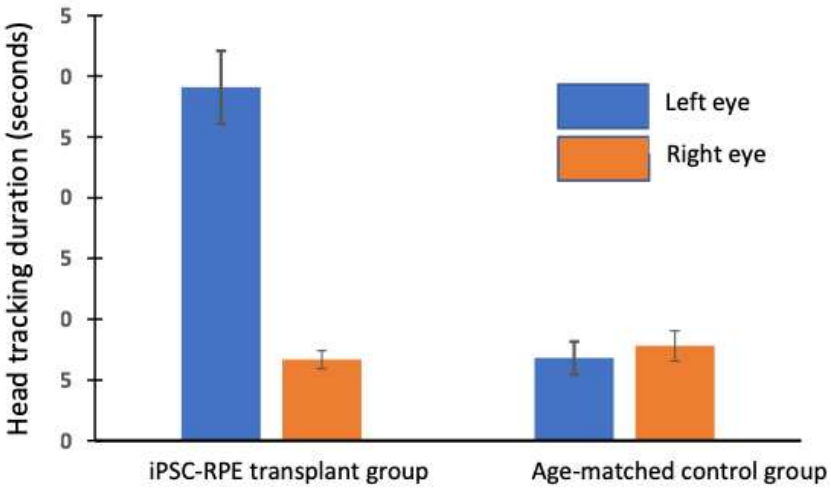

 doi:10.20944/preprints202109.0340.v1

Figure 6. OKN testing data based on the duration of head-tracking recorded from 4-month-old immunodeficient RCS rats (± SE). The data shows improved head-tracking response in the iPSC-RPE transplanted left eyes (n=12) compared to the non-transplanted eyes and age-matched control rats (n=5).

4. Discussion

Ongoing multicentral clinical studies have proven that stem cell-derived RPE transplantation is a practical option to restore failing vision in retinal dystrophies [3,12,17,20,28,32–35]. Previous animal studies and pilot data from our Phase l/ ll clinical studies demonstrated the feasibility of using ultrathin parylene as a bio membrane for hESC-RPE growth and subretinal implantation [12,15,17,36]. Compared to hESC-RPE, using iPSC derived RPE is considered more advantageous due to the possibility to generate sufficient number of autologous RPE cells that strongly resembles primary human RPEs and because of its potential to minimize issues associated with immune rejection. Based on this, the present study evaluated the long-term benefits of polarized iPSC-RPE cells grown on ultrathin parylene membrane that can act as an artificial Bruch's membrane. The ability of such implants to support transplant survival and viability of the host photoreceptors to preserve visual function is demonstrated in a new immunodeficient RCS rat model.

Majority of the previous iPSC-RPE transplantation studies were conducted in immunosuppressed animal models and assessments were made only for short duration that may not be sufficient to extrapolate into long-term implications [25,42–45]. Hence, in the present study, transplant effects were analysed in a new immunodeficient RCS rat model and assessments were conducted up to one year after implantation. The results from this study demonstrated the safety and potential bioactivity of the iPSC-RPE implant both during the short term (1-4 month) investigation and long-term investigation (11-month study). Based on histology assessments, good coverage of the implanted iPSC-RPE on the parylene membrane was observed in the majority of eyes up to 4-months post-implantation along with improvement in visual function confirmed by OKN testing. In our long-term studies (11-months post transplantation), iPSC-RPE survival and phagocytic function was observed only in less than 50% of the transplanted rats (7/15). In another report, loss of transplanted iPSC- RPE in RCS rats, immunosuppressed by oral administration of cyclosporin, was observed at 13 weeks post-transplantation [45]. Based on the available data, loss of transplanted RPE over the course of time and alteration in the monolayer structure can be related to immune reaction to xenografts [28,32,48].

Previous studies have shown that, survival and integration of transplanted ESC-RPEs in the pathologic environment of diseased retina is challenging due to it being prone to attack by macrophages [15]. CD 68 expression has been reported in studies using hESC-RPE transplantation and hESC-RPE cell suspension injections in immunosuppressed RCS rats [15, 49,50]. In the present investigation, we used immunodeficient RCS rats to reduce the immunological issues. However, signs of inflammation and microglia activation has been previously reported in immunodeficient RCS rats [40]. Hence, we used CD68 as a marker for assessing reactive microglia in the transplanted eyes. In our long-term studies, some CD 68 expression was observed in the implants and in areas adjacent to them (Fig 5d). However, this phenomenon was not observed at the early timepoint (1-month post-implantation, see supplementary Figure 1). This suggests that reactive microglia/macrophages can play a role in the loss of transplanted RPEs at later timepoint. In contrast to the above reports, recent study by Zhu et.al suggested that iPSC-PRE cell suspension injection can lower the microglial activation (CD68 expression) in rd10 mice [33]. The discrepancies study outcome can be related to the differences in the animal models used, time points in which CD68 staining was conducted and the cell types used for transplantation experiments.

Glial fibrillary acid protein (GFAP) expression which is known to occur in response to retinal injuries [51] can be also suggested for a role in transplant loss in the 11-month study group. However, GFAP expression in the above study group was found mostly adjacent to the inner nuclear region, choroid area and ganglionic layer, which is away from the implant area. Since this GFP expression pattern is comparable to that of the non-transplanted control eyes [52], the presence of GFAP cannot be correlated to the loss of transplanted iPSC-RPEs.

 doi:10.20944/preprints202109.0340.v1

In some of our transplanted eyes, the iPSC-RPEs developed into cell clumps on the surface of the parylene membrane (Fig. 3d). Previous studies suggested that when RPE transplant fail to establish a monolayer and form cell clumps, its survival will be poor and the cells will not be capable of performing normal RPE functions [46,47]. Based on this finding, it suggests that implants may need to be microscopically examined for potential signs of clumping prior to subretinal implantation.

The cell clump formation observed in about 20% implanted eyes (long-term study group) might have occurred even after transplantation due to cell migration. Cell migration is mainly attributed to loss of RPE tight junctions [53]. This can lead to loss of cell to cell contact and anchorage dependence that are critical for RPE survival and functionality [54]. Emerging evidence demonstrates that RPE cells can be less differentiated and undergo epithelial-mesenchymal transition (EMT) and enhanced migration in retinal degenerative diseases including macular degenerations and proliferative vitreoretinopathy [56–59]. Such transition is also reported in higher passage RPEs during *in vitro* observations [60,61]. Immunostaining of transplanted eyes from 11-month study group revealed the presence of two classic mesenchymal cell markers namely α SMA and vimentin, especially in areas of the parylene membrane where loss of RPE expression was noticed. Transition to mesenchymal fate may cause loss of tight junctions and reduced cell adherence to parylene membrane that can lead to a fibroblastic phenotype [53,54]. According to Zhou et. al [55], RPE cells retain the reprogramming capacity to move along a continuum between polarized epithelial cells and mesenchymal cells. This shift towards a mesenchymal phenotype can be defined as RPE dysfunction [55]. This change of RPE characteristics can cause senescence/ fibrosis, eventually resulting in loss of transplanted cells. In our transplanted rats, the expression of EMT markers were not evident at the earlier time point (1-month study group) when RPE survival was more robust (supplementary Figure 2). Further studies are needed to identify the exact time point at which the EMT markers are expressed to determine whether changes in the iPSC-RPEs takes place only in the long-term post-implantation period.

The RCS retina is widely known for its acute reactions to surgical interventions. Surgical trauma that are severe in the rat eyes due to its small size can lead to increased tissue reactions in the implanted area. In support for this, mild inflammation and peri-membrane fibrosis were visible around majority of the implants in which RPE monolayer was lost. It may be noted that, although the immunodeficient RCS rat is T- cell deficient, they possess bone marrow-dependent B cells and natural killer (NK) cells. All the above factors can contribute to the loss of transplanted iPSC-RPE cells.

In the long-term study group (11-month post-implantation), the visual functional preservation (based on SC electrophysiology) was correlated to the survival of the transplanted iPSC-RPE. However, no considerable OKN visual activities were observed these rats at this time point. Previously, in hESC-RPE implanted immunosuppressed RCS rats, such progressive loss of OKN responses has been reported [17]. Improved OKN visual activities observed at earlier time point (4 month) can have contribution from residual photoreceptors present in the RCS retina. When the photoreceptor degeneration is more advanced, the transplant benefit can be limited to a very small area of the retina and its contribution may not be strong enough to evoke measurable head-tracking activities.

In conclusion, the present study demonstrated the survival and functionality of iPSC-RPE transplanted as a polarized monolayer on a non-degradable substrate containing similarities to an artificial Bruch's membrane. The transplant benefits are higher during earlier post-implantation period. Progressive deterioration of the transplant benefits observed in this study was correlated with the loss of transplanted iPSC-RPEs. The immune reactions and subretinal fibrosis can be considered as the major cause for the loss of transplanted iPSC-RPE. From a clinical perspective, many of these adverse effects can be less severe in human due to the differences in the eye architecture, surgical procedures, and the nature of the disease microenvironment. Also, in human eyes, easy application of target specific and effective immune suppressants can help to reduce potential immunological reactions.

Author Contributions: Conceptualization, Biju B. Thomas.; Methodology, Danhong Zhu, Deepthi S. Rajendran Nair, Juan Carlos Martinez Camarillo, Biju B. Thomas.; Validation Biju B. Thomas, Kapil Bharti, Mark S. Humayun, Juan Carlos Martinez Camarillo, Deepthi S. Rajendran Nair.;

Resources, Biju B. Thomas, Kapil Bharti, Mark S. Humayun; Writing – Original Draft Preparation, Deepthi S. Rajendran Nair, Biju B. Thomas, Writing – Review & Editing, Biju B. Thomas, Deepthi S. Rajendran Nair, Danhong Zhu, Juan Carlos Martinez Camarillo, Kapil Bharti, Mark S. Humayun.; Supervision Biju B. Thomas, Funding Acquisition, Biju B. Thomas

Funding: This study was funded by the grant from Bright Focus Foundation (M2016186, Thomas, PI). Research reported in this publication was supported by the National Eye Institute of the National Institutes of Health under Award Number P30EY029220. CIRM (California Institute for Regenerative Medicine) grants (DISC1-09912 PI- Thomas, DR3-07438- PI- Humayun), Unrestricted Grant to the Department of Ophthalmology from Research to Prevent Blindness, New York, NY. The content is solely the responsibility of the authors and does not necessarily represent the official views of the National Institutes of Health

Institutional Review Board Statement: All experiments were approved by the University of Southern California Animal Care and Use Committee and were performed in accordance with the National Institute of Health *Guide for the Care and Use of Laboratory Animals* and the ARVO Statement for the Use of Animals in Ophthalmic and Vision Research.

Informed Consent Statement: Not Applicable
Data Availability Statement: Data used to support the findings in this study are contained within this article and Supplementary Material

Acknowledgments: We thank Dr. Jane Lebkowski (president R&D at Regenerative Patch Technologies, Portola Valley, CA) for critically reviewing the manuscript. The authors want to thank Xiaopeng Wang (USC) for histological processing of the tissue samples.

Conflicts of Interest: Regenerative Patch Technologies: MSH and DZ have proprietary interests in the culture of RPE on ultrathin parylene

 doi:10.20944/preprints202109.0340.v1

Appendix A

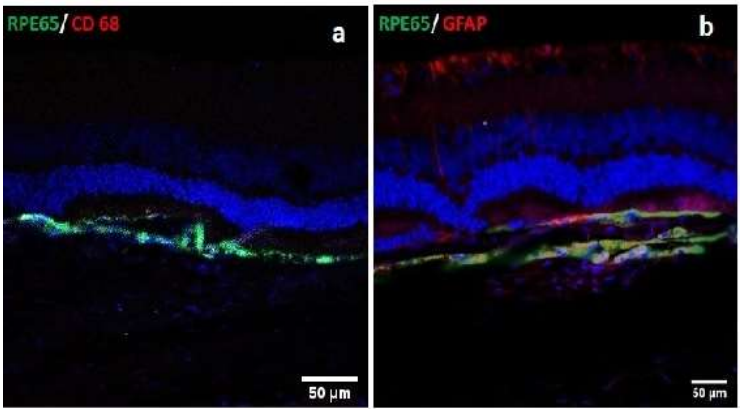

Figure A1. Representative images of immunodeficient RCS rat retinas implanted with iPSC-RPE monolayer (shown by RPE65 expression) cultured on a parylene membrane assessed at 1-month post implantation. Additional labelling of the retina sections was performed for expression of (a) CD68 (macrophages/ microglia) and (b) GFAP (glial cells).

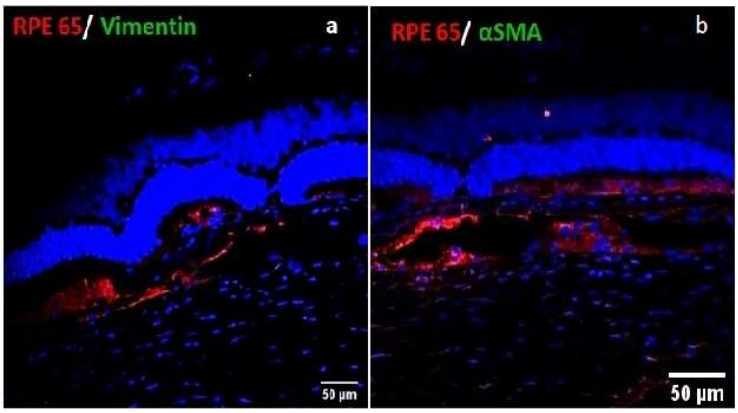

Figure A2. Representative images of immunodeficient RCS rat retinas implanted with iPSC-RPE monolayer (shown by RPE65 expression) cultured on a parylene membrane assessed at 1-month post implantation. Additional labelling of the retina sections was performed for expression of classical mesenchymal markers(a) vimentin and (b) α smooth muscle actin (α SMA).

References

References must be numbered in order of appearance in the text (including citations in tables and legends) and listed individually at the end of the manuscript. We recommend preparing the references with a bibliography software package, such as EndNote, ReferenceManager or Zotero to avoid typing mistakes and duplicated references. Include the digital object identifier (DOI) for all references where available.

Citations and references in the Supplementary Materials are permitted provided that they also appear in the reference list here.

In the text, reference numbers should be placed in square brackets [ ] and placed before the punctuation; for example [1], [1–3] or [1,3]. For embedded citations in the text with pagination, use both parentheses and brackets to indicate the reference number and page numbers; for example [5] (p. 10), or [6] (pp. 101–105).

1. Foltz, L.P.; Clegg, D.O. Rapid, Directed Differentiation of Retinal Pigment Epithelial Cells from Human Embryonic or Induced Pluripotent Stem Cells. *J. Vis. Exp. JoVE* **2017**, doi:10.3791/56274.
2. Klimanskaya, I.; Hipp, J.; Rezai, K.A.; West, M.; Atala, A.; Lanza, R. Derivation and Comparative Assessment of Retinal Pigment Epithelium from Human Embryonic Stem Cells Using Transcriptomics. *Cloning Stem Cells* **2004**, *6*, 217–245, doi:10.1089/clo.2004.6.217.
3. Lund, R.D.; Wang, S.; Klimanskaya, I.; Holmes, T.; Ramos-Kelsey, R.; Lu, B.; Girman, S.; Bischoff, N.; Sauvé, Y.; Lanza, R. Human Embryonic Stem Cell-Derived Cells Rescue Visual Function in Dystrophic RCS Rats. *Cloning Stem Cells* **2006**, *8*, 189–199, doi:10.1089/clo.2006.8.189.
4. Idelson, M.; Alper, R.; Obolensky, A.; Ben-Shushan, E.; Hemo, I.; Yachimovich-Cohen, N.; Khaner, H.; Smith, Y.; Wiser, O.; Gropp, M.; et al. Directed Differentiation of Human Embryonic Stem Cells into Functional Retinal Pigment Epithelium Cells. *Cell Stem Cell* **2009**, *5*, 396–408, doi:10.1016/j.stem.2009.07.002.
5. Rowland, T.J.; Blaschke, A.J.; Buchholz, D.E.; Hikita, S.T.; Johnson, L.V.; Clegg, D.O. Differentiation of Human Pluripotent Stem Cells to Retinal Pigmented Epithelium in Defined Conditions Using Purified Extracellular Matrix Proteins. *J. Tissue Eng. Regen. Med.* **2013**, *7*, 642–653, doi:10.1002/term.1458.
6. Hazim, R.A.; Karumbayaram, S.; Jiang, M.; Dimashkie, A.; Lopes, V.S.; Li, D.; Burgess, B.L.; Vijayaraj, P.; Alva-Ornelas, J.A.; Zack, J.A.; et al. Differentiation of RPE Cells from Integration-Free IPS Cells and Their Cell Biological Characterization. *Stem Cell Res. Ther.* **2017**, *8*, doi:10.1186/s13287-017-0652-9.
7. D'Antonio-Chronowska, A.; D'Antonio, M.; Frazer, K.A. In Vitro Differentiation of Human IPSC-Derived Retinal Pigment Epithelium Cells (IPSC-RPE). *Bio-Protoc.* **2019**, *9*, e3469–e3469.
8. Buchholz, D.E.; Hikita, S.T.; Rowland, T.J.; Friedrich, A.M.; Hinman, C.R.; Johnson, L.V.; Clegg, D.O. Derivation of Functional Retinal Pigmented Epithelium from Induced Pluripotent Stem Cells. *STEM CELLS* **2009**, *27*, 2427–2434, doi:https://doi.org/10.1002/stem.189.
9. Sharma, R.; Khristov, V.; Rising, A.; Jha, B.S.; Dejene, R.; Hotaling, N.; Li, Y.; Stoddard, J.; Stankewicz, C.; Wan, Q.; et al. Clinical-Grade Stem Cell-Derived Retinal Pigment Epithelium Patch Rescues Retinal Degeneration in Rodents and Pigs. *Sci. Transl. Med.* **2019**, *11*, doi:10.1126/scitranslmed.aat5580.
10. Schwartz, S.D.; Tan, G.; Hosseini, H.; Nagiel, A. Subretinal Transplantation of Embryonic Stem Cell-Derived Retinal Pigment Epithelium for the Treatment of Macular Degeneration: An Assessment at 4 Years. *Invest. Ophthalmol. Vis. Sci.* **2016**, *57*, ORSFc1-9, doi:10.1167/iovs.15-18681.
11. Schwartz, S.D.; Hubschman, J.-P.; Heilwell, G.; Franco-Cardenas, V.; Pan, C.K.; Ostrick, R.M.; Mickunas, E.; Gay, R.; Klimanskaya, I.; Lanza, R. Embryonic Stem Cell Trials for Macular Degeneration: A Preliminary Report. *Lancet Lond. Engl.* **2012**, *379*, 713–720, doi:10.1016/S0140-6736(12)60028-2.
12. Kashani, A.H.; Lebkowski, J.S.; Rahhal, F.M.; Avery, R.L.; Salehi-Had, H.; Dang, W.; Lin, C.-M.; Mitra, D.; Zhu, D.; Thomas, B.B.; et al. A Bioengineered Retinal Pigment Epithelial Monolayer for Advanced, Dry Age-Related Macular Degeneration. *Sci. Transl. Med.* **2018**, *10*, doi:10.1126/scitranslmed.aao4097.
13. da Cruz, L.; Fynes, K.; Georgiadis, O.; Kerby, J.; Luo, Y.H.; Ahmado, A.; Vernon, A.; Daniels, J.T.; Nommiste, B.; Hasan, S.M.; et al. Phase 1 Clinical Study of an Embryonic Stem Cell-Derived Retinal Pigment Epithelium Patch in Age-Related Macular Degeneration. *Nat. Biotechnol.* **2018**, *36*, 328–337, doi:10.1038/nbt.4114.
14. Mandai, M.; Watanabe, A.; Kurimoto, Y.; Hirami, Y.; Morinaga, C.; Daimon, T.; Fujihara, M.; Akimaru, H.; Sakai, N.; Shibata, Y.; et al. Autologous Induced Stem-Cell–Derived Retinal Cells for Macular Degeneration. *N. Engl. J. Med.* **2017**, *376*, 1038–1046, doi:10.1056/NEJMoa1608368.

15. Diniz, B.; Thomas, P.; Thomas, B.; Ribeiro, R.; Hu, Y.; Brant, R.; Ahuja, A.; Zhu, D.; Liu, L.; Koss, M.; et al. Subretinal Implantation of Retinal Pigment Epithelial Cells Derived from Human Embryonic Stem Cells: Improved Survival When Implanted as a Monolayer. *Invest. Ophthalmol. Vis. Sci.* **2013**, *54*, 5087–5096, doi:10.1167/iovs.12-11239.
16. Hu, Y.; Liu, L.; Lu, B.; Zhu, D.; Ribeiro, R.; Diniz, B.; Thomas, P.B.; Ahuja, A.K.; Hinton, D.R.; Tai, Y.-C.; et al. A Novel Approach for Subretinal Implantation of Ultrathin Substrates Containing Stem Cell-Derived Retinal Pigment Epithelium Monolayer. *Ophthalmic Res.* **2012**, *48*, 186–191, doi:10.1159/000338749.
17. Thomas, B.B.; Zhu, D.; Zhang, L.; Thomas, P.B.; Hu, Y.; Nazari, H.; Stefanini, F.; Falabella, P.; Clegg, D.O.; Hinton, D.R.; et al. Survival and Functionality of HESC-Derived Retinal Pigment Epithelium Cells Cultured as a Monolayer on Polymer Substrates Transplanted in RCS Rats. *Invest. Ophthalmol. Vis. Sci.* **2016**, *57*, 2877–2887, doi:10.1167/iovs.16-19238.
18. Kashani, A.H.; Lebkowski, J.S.; Rahhal, F.M.; Avery, R.L.; Salehi-Had, H.; Dang, W.; Lin, C.-M.; Mitra, D.; Zhu, D.; Thomas, B.B.; et al. A Bioengineered Retinal Pigment Epithelial Monolayer for Advanced, Dry Age-Related Macular Degeneration. *Sci. Transl. Med.* **2018**, *10*, doi:10.1126/scitranslmed.aao4097.
19. Takagi, S.; Mandai, M.; Gocho, K.; Hirami, Y.; Yamamoto, M.; Fujihara, M.; Sugita, S.; Kurimoto, Y.; Takahashi, M. Evaluation of Transplanted Autologous Induced Pluripotent Stem Cell-Derived Retinal Pigment Epithelium in Exudative Age-Related Macular Degeneration. *Ophthalmol. Retina* **2019**, *3*, 850–859, doi:10.1016/j.oret.2019.04.021.
20. Sugita, S.; Mandai, M.; Hirami, Y.; Takagi, S.; Maeda, T.; Fujihara, M.; Matsuzaki, M.; Yamamoto, M.; Iseki, K.; Hayashi, N.; et al. HLA-Matched Allogeneic IPS Cells-Derived RPE Transplantation for Macular Degeneration. *J. Clin. Med.* **2020**, *9*, 2217, doi:10.3390/jcm9072217.
21. Sugita, S.; Iwasaki, Y.; Makabe, K.; Kamao, H.; Mandai, M.; Shiina, T.; Ogasawara, K.; Hirami, Y.; Kurimoto, Y.; Takahashi, M. Successful Transplantation of Retinal Pigment Epithelial Cells from MHC Homozygote IPSCs in MHC-Matched Models. *Stem Cell Rep.* **2016**, *7*, 635–648, doi:10.1016/j.stemcr.2016.08.010.
22. Sugita, S.; Mandai, M.; Hirami, Y.; Takagi, S.; Maeda, T.; Fujihara, M.; Matsuzaki, M.; Yamamoto, M.; Iseki, K.; Hayashi, N.; et al. HLA-Matched Allogeneic IPS Cells-Derived RPE Transplantation for Macular Degeneration. *J. Clin. Med.* **2020**, *9*, doi:10.3390/jcm9072217.
23. Mandai, M.; Watanabe, A.; Kurimoto, Y.; Hirami, Y.; Morinaga, C.; Daimon, T.; Fujihara, M.; Akimaru, H.; Sakai, N.; Shibata, Y.; et al. Autologous Induced Stem-Cell-Derived Retinal Cells for Macular Degeneration. *N. Engl. J. Med.* **2017**, *376*, 1038–1046, doi:10.1056/NEJMoa1608368.
24. Garber, K. RIKEN Suspends First Clinical Trial Involving Induced Pluripotent Stem Cells. *Nat. Biotechnol.* **2015**, *33*, 890–891, doi:10.1038/nbt0915-890.
25. Sharma, R.; Khristov, V.; Rising, A.; Jha, B.S.; Dejene, R.; Hotaling, N.; Li, Y.; Stoddard, J.; Stankewicz, C.; Wan, Q.; et al. Clinical-Grade Stem Cell–Derived Retinal Pigment Epithelium Patch Rescues Retinal Degeneration in Rodents and Pigs. *Sci. Transl. Med.* **2019**, *11*, doi:10.1126/scitranslmed.aat5580.
26. Kanemura, H.; Go, M.J.; Shikamura, M.; Nishishita, N.; Sakai, N.; Kamao, H.; Mandai, M.; Morinaga, C.; Takahashi, M.; Kawamata, S. Tumorigenicity Studies of Induced Pluripotent Stem Cell (IPSC)-Derived Retinal Pigment Epithelium (RPE) for the Treatment of Age-Related Macular Degeneration. *PLOS ONE* **2014**, *9*, e85336, doi:10.1371/journal.pone.0085336.
27. Zhang, H.; Su, B.; Jiao, L.; Xu, Z.-H.; Zhang, C.-J.; Nie, J.; Gao, M.-L.; Zhang, Y.V.; Jin, Z.-B. Transplantation of GMP-Grade Human IPSC-Derived Retinal Pigment Epithelial Cells in Rodent Model: The First Pre-Clinical Study for Safety and Efficacy in China. *Ann. Transl. Med.* **2021**, *9*, 245, doi:10.21037/atm-20-4707.
28. Sohn, E.; Jiao, C.; Kaalberg, E.; Cranston, C.; Mullins, R.; Stone, E.; Budd; Tucker, B. Allogenic IPSC-Derived RPE Cell Transplants Induce Immune Response in Pigs: A Pilot Study. *Sci. Rep.* **2015**, *5*, doi:10.1038/srep11791.
29. Westenskow, P.D.; Bucher, F.; Bravo, S.; Kurihara, T.; Feitelberg, D.; Paris, L.P.; Aguilar, E.; Lin, J.H.; Friedlander, M. IPSC-Derived Retinal Pigment Epithelium Allografts Do Not Elicit Detrimental Effects in Rats: A Follow-Up Study. *Stem Cells Int.* **2016**, *2016*, doi:10.1155/2016/8470263.
30. Maruotti, J.; Sripathi, S.R.; Bharti, K.; Fuller, J.; Wahlin, K.J.; Ranganathan, V.; Sluch, V.M.; Berlinicke, C.A.; Davis, J.; Kim, C.; et al. 30-Molecule–Directed, Efficient Generation of Retinal Pigment Epithelium from Human Pluripotent Stem Cells. *Proc. Natl. Acad. Sci.* **2015**, *112*, 10950–10955, doi:10.1073/pnas.1422818112.
31. Thomas, B.B.; Zhu, D.; Lin, T.-C.; Kim, Y.C.; Seiler, M.J.; Martinez-Camarillo, J.C.; Lin, B.; Shad, Y.; Hinton, D.R.; Humayun, M.S. A New Immunodeficient Retinal Dystrophic Rat Model for Transplantation Studies Using Human-Derived Cells. *Graefes Arch. Clin. Exp. Ophthalmol. Albrecht Von Graefes Arch. Klin. Exp. Ophthalmol.* **2018**, *256*, 2113–2125, doi:10.1007/s00417-018-4134-2.
32. McGill, T.J.; Stoddard, J.; Renner, L.M.; Messaoudi, I.; Bharti, K.; Mitalipov, S.; Lauer, A.; Wilson, D.J.; Neuringer, M. Allogeneic IPSC-Derived RPE Cell Graft Failure Following Transplantation Into the Subretinal Space in Nonhuman Primates. *Invest. Ophthalmol. Vis. Sci.* **2018**, *59*, 1374–1383, doi:10.1167/iovs.17-22467.
33. Zhu, D.; Xie, M.; Gademann, F.; Cao, J.; Wang, P.; Guo, Y.; Zhang, L.; Su, T.; Zhang, J.; Chen, J. Protective Effects of Human IPS-Derived Retinal Pigmented Epithelial Cells on Retinal Degenerative Disease. *Stem Cell Res. Ther.* **2020**, *11*, 98, doi:10.1186/s13287-020-01608-8.
34. Mandai, M.; Fujii, M.; Hashiguchi, T.; Sunagawa, G.A.; Ito, S.; Sun, J.; Kaneko, J.; Sho, J.; Yamada, C.; Takahashi, M. IPSC-Derived Retina Transplants Improve Vision in Rd1 End-Stage Retinal-Degeneration Mice. *Stem Cell Rep.* **2017**, *8*, 69–83, doi:10.1016/j.stemcr.2016.12.008.

35. Sugita, S.; Iwasaki, Y.; Makabe, K.; Kamao, H.; Mandai, M.; Shiina, T.; Ogasawara, K.; Hirami, Y.; Kurimoto, Y.; Takahashi, M. Successful Transplantation of Retinal Pigment Epithelial Cells from MHC Homozygote IPSCs in MHC-Matched Models. *Stem Cell Rep.* **2016**, *7*, 635–648, doi:10.1016/j.stemcr.2016.08.010.
36. Koss, M.J.; Falabella, P.; Stefanini, F.R.; Pfister, M.; Thomas, B.B.; Kashani, A.H.; Brant, R.; Zhu, D.; Clegg, D.O.; Hinton, D.R.; et al. Subretinal Implantation of a Monolayer of Human Embryonic Stem Cell-Derived Retinal Pigment Epithelium: A Feasibility and Safety Study in Yucatán Minipigs. *Graefes Arch. Clin. Exp. Ophthalmol. Albrecht Von Graefes Arch. Klin. Exp. Ophthalmol.* **2016**, *254*, 1553–1565, doi:10.1007/s00417-016-3386-y.
37. Sharma, R.; Khristov, V.; Rising, A.; Jha, B.S.; Dejene, R.; Hotaling, N.; Li, Y.; Stoddard, J.; Stankewicz, C.; Wan, Q.; et al. Clinical-Grade Stem Cell–Derived Retinal Pigment Epithelium Patch Rescues Retinal Degeneration in Rodents and Pigs. *Sci. Transl. Med.* **2019**, *11*, doi:10.1126/scitranslmed.aat5580.
38. Cooper, A.E.; Cho, J.-H.; Menges, S.; Masood, S.; Xie, J.; Yang, J.; Klassen, H. Immunosuppressive Treatment Can Alter Visual Performance in the Royal College of Surgeons Rat. *J. Ocul. Pharmacol. Ther. Off. J. Assoc. Ocul. Pharmacol. Ther.* **2016**, *32*, 296–303, doi:10.1089/jop.2015.0134.
39. Priore, L.V.D.; Ishida, O.; Johnson, E.W.; Sheng, Y.; Jacoby, D.B.; Geng, L.; Tezel, T.H.; Kaplan, H.J. Triple Immune Suppression Increases Short-Term Survival of Porcine Fetal Retinal Pigment Epithelium Xenografts. *Invest. Ophthalmol. Vis. Sci.* **2003**, *44*, 4044–4053, doi:10.1167/iovs.02-1175.
40. Thomas, B.B.; Zhu, D.; Lin, T.-C.; Kim, Y.C.; Seiler, M.J.; Martinez-Camarillo, J.C.; Lin, B.; Shad, Y.; Hinton, D.R.; Humayun, M.S. A New Immunodeficient Retinal Dystrophic Rat Model for Transplantation Studies Using Human-Derived Cells. *Graefes Arch. Clin. Exp. Ophthalmol.* **2018**, *256*, 2113–2125, doi:10.1007/s00417-018-4134-2.
41. Siminoff R, Schwassmann HO, Kruger L. An electrophysiological study of the visual projection to the superior colliculus of the rat. J Comp Neurol. 1966 Aug;127(4):435–44.
42. Shrestha, R.; Wen, Y.-T.; Tsai, R.-K. Effective Differentiation and Biological Characterization of Retinal Pigment Epithelium Derived from Human Induced Pluripotent Stem Cells. *Curr. Eye Res.* **2020**, *45*, 1155–1167, doi:10.1080/02713683.2020.1722180.
43. Zhu, D.; Xie, M.; Gademann, F.; Cao, J.; Wang, P.; Guo, Y.; Zhang, L.; Su, T.; Zhang, J.; Chen, J. Protective Effects of Human IPS-Derived Retinal Pigmented Epithelial Cells on Retinal Degenerative Disease. *Stem Cell Res. Ther.* **2020**, *11*, 98, doi:10.1186/s13287-020-01608-8.
44. Fujii, S.; Sugita, S.; Futatsugi, Y.; Ishida, M.; Edo, A.; Makabe, K.; Kamao, H.; Iwasaki, Y.; Sakaguchi, H.; Hirami, Y.; et al. A Strategy for Personalized Treatment of IPS-Retinal Immune Rejections Assessed in Cynomolgus Monkey Models. *Int. J. Mol. Sci.* **2020**, *21*, doi:10.3390/ijms21093077.
45. Carr, A.-J.; Vugler, A.A.; Hikita, S.T.; Lawrence, J.M.; Gias, C.; Chen, L.L.; Buchholz, D.E.; Ahmado, A.; Semo, M.; Smart, M.J.K.; et al. Protective Effects of Human IPS-Derived Retinal Pigment Epithelium Cell Transplantation in the Retinal Dystrophic Rat. *PLOS ONE* **2009**, *4*, e8152, doi:10.1371/journal.pone.0008152.
46. Algvere, P.V.; Gouras, P.; Dafgård Kopp, E. Long-Term Outcome of RPE Allografts in Non-Immunosuppressed Patients with AMD. *Eur. J. Ophthalmol.* **1999**, *9*, 217–230, doi:10.1177/112067219900900310.
47. Sheridan, C.M.; Mason, S.; Pattwell, D.M.; Kent, D.; Grierson, I.; Williams, R. Replacement of the RPE Monolayer. *Eye* **2009**, *23*, 1910–1915, doi:10.1038/eye.2008.420.
48. Petrus-Reurer, S.; Romano, M.; Howlett, S.; Jones, J.L.; Lombardi, G.; Saeb-Parsy, K. Immunological Considerations and Challenges for Regenerative Cellular Therapies. *Commun. Biol.* **2021**, *4*, 798, doi:10.1038/s42003-021-02237-4.
49. Ilmarinen, T.; Hiidenmaa, H.; Kööbi, P.; Nymark, S.; Sorkio, A.; Wang, J.-H.; Stanzel, B.V.; Thieltges, F.; Alajuuma, P.; Oksala, O.; et al. Ultrathin Polyimide Membrane as Cell Carrier for Subretinal Transplantation of Human Embryonic Stem Cell Derived Retinal Pigment Epithelium. *PLOS ONE* **2015**, *10*, e0143669, doi:10.1371/journal.pone.0143669.
50. Karlstetter, M.; Scholz, R.; Rutar, M.; Wong, W.T.; Provis, J.M.; Langmann, T. Retinal Microglia: Just Bystander or Target for Therapy? *Prog. Retin. Eye Res.* **2015**, *45*, 30–57, doi:10.1016/j.preteyeres.2014.11.004.
51. Ekström, P.; Sanyal, S.; Narfström, K.; Chader, G.; Veen, T. Accumulation of Glial Fibrillary Acidic Protein in Muller Radial Glia during Retinal Degeneration. *Invest. Ophthalmol. Vis. Sci.* **1988**, *29*, 1363–71.
52. Di Pierdomenico, J.; García-Ayuso, D.; Pinilla, I.; Cuenca, N.; Vidal-Sanz, M.; Agudo-Barriuso, M.; Villegas-Pérez, M.P. Early Events in Retinal Degeneration Caused by Rhodopsin Mutation or Pigment Epithelium Malfunction: Differences and Similarities. *Front. Neuroanat.* **2017**, *0*, doi:10.3389/fnana.2017.00014.
53. Carlsson, E.; Supharattanasitthi, W.; Jackson, M.; Paraoan, L. Increased Rate of Retinal Pigment Epithelial Cell Migration and Pro-Angiogenic Potential Ensuing From Reduced Cystatin C Expression. *Invest. Ophthalmol. Vis. Sci.* **2020**, *61*, 9–9, doi:10.1167/iovs.61.2.9.
54. White, C.; DiStefano, T.; Olabisi, R. The Influence of Substrate Modulus on Retinal Pigment Epithelial Cells. *J. Biomed. Mater. Res. A* **2017**, *105*, 1260–1266, doi:10.1002/jbm.a.35992.
55. Zhou, M.; Geathers, J.S.; Grillo, S.L.; Weber, S.R.; Wang, W.; Zhao, Y.; Sundstrom, J.M. Role of Epithelial-Mesenchymal Transition in Retinal Pigment Epithelium Dysfunction. *Front. Cell Dev. Biol.* **2020**, *0*, doi:10.3389/fcell.2020.00501.
56. Lamouille, S.; Xu, J.; Derynck, R. Molecular Mechanisms of Epithelial–Mesenchymal Transition. *Nat. Rev. Mol. Cell Biol.* **2014**, *15*, 178–196, doi:10.1038/nrm3758.
57. Ferrer-vaquer, A.; Viotti, M.; Hadjantonakis, A.-K. Transitions between Epithelial and Mesenchymal States and the Morphogenesis of the Early Mouse Embryo. *Cell Adhes. Migr.* **2010**, *4*, 447–457, doi:10.4161/cam.4.3.10771.

58. Tamiya, S.; Kaplan, H.J. Role of Epithelial-Mesenchymal Transition in Proliferative Vitreoretinopathy. *Exp. Eye Res.* **2016**, *142*, 26–31, doi:10.1016/j.exer.2015.02.008.
59. Ghosh, S.; Shang, P.; Terasaki, H.; Stepicheva, N.; Hose, S.; Yazdankhah, M.; Weiss, J.; Sakamoto, T.; Bhutto, I.A.; Xia, S.; et al. A Role for BA3/A1-Crystallin in Type 2 EMT of RPE Cells Occurring in Dry Age-Related Macular Degeneration. *Invest. Ophthalmol. Vis. Sci.* **2018**, *59*, AMD104–AMD113, doi:10.1167/iovs.18-24132.
60. Zou, H.; Shan, C.; Ma, L.; Liu, J.; Yang, N.; Zhao, J. Polarity and Epithelial-Mesenchymal Transition of Retinal Pigment Epithelial Cells in Proliferative Vitreoretinopathy. *PeerJ* **2020**, *8*, e10136, doi:10.7717/peerj.10136.
61. Shu, D.Y.; Butcher, E.; Saint-Geniez, M. EMT and EndMT: Emerging Roles in Age-Related Macular Degeneration. *Int. J. Mol. Sci.* **2020**, *21*, 4271, doi:10.3390/ijms21124271.